ORIGINAL ARTICLE

Orchestration of Hippocampal Information Encoding by the Piriform Cortex

Christina Strauch[1,2] and Denise Manahan-Vaughan[1,2]

[1]Department of Neurophysiology, Medical Faculty and [2]International Graduate School for Neuroscience, Ruhr University Bochum, Universitaetsstr. 150, 44780 Bochum, Germany

Address correspondence to Denise Manahan-Vaughan, Department of Neurophysiology, Medical Faculty, Ruhr University Bochum, MA 4/150, Universitaetsstr. 150, 44780 Bochum, Germany. Email: dmv-igsn@rub.de.

Abstract

The hippocampus utilizes olfactospatial information to encode sensory experience by means of synaptic plasticity. Odor exposure is also a potent impetus for hippocampus-dependent memory retrieval. Here, we explored to what extent the piriform cortex directly impacts upon hippocampal information processing and storage. In behaving rats, test-pulse stimulation of the anterior piriform cortex (aPC) evoked field potentials in the dentate gyrus (DG). Patterned stimulation of the aPC triggered both long-term potentiation (LTP > 24 h) and short-term depression (STD), in a frequency-dependent manner. Dual stimulation of the aPC and perforant path demonstrated subordination of the aPC response, which was nonetheless completely distinct in profile to perforant path-induced DG plasticity. Correspondingly, patterned aPC stimulation resulted in somatic immediate early gene expression in the DG that did not overlap with responses elicited by perforant path stimulation. Our results support that the piriform cortex engages in specific control of hippocampal information processing and encoding. This process may underlie the unique role of olfactory cues in information encoding and retrieval of hippocampus-dependent associative memories.

Key words: dentate gyrus, hippocampus, in vivo, olfactory system, rodent, synaptic plasticity

Introduction

The hippocampus integrates information derived from multiple sensory and cognitive sources to enable generation of associative and explicit memory (Squire 1992; Squire et al. 2004; Bird and Burgess 2008; Neves et al. 2008). In rodents, encoding of this kind is enabled by synaptic plasticity, whereby spatial experience in the visual (Kemp and Manahan-Vaughan 2004), auditory (Dietz and Manahan-Vaughan 2017), and olfactory modalities (André and Manahan-Vaughan 2013) facilitate the expression of very long-term forms of hippocampal synaptic plasticity that persist for days and weeks.

The novelist Marcel Proust (†1922) was one of the first to draw attention to the potency of olfactory cues as instigators of the retrieval of complex (and believed to be forgotten) explicit memories. This observation was subsequently scrutinized in detail by cognitive scientists (Eichenbaum and Robitsek 2009; Jacobs 2012; Jacobs et al. 2015). On the empirical level, it has been shown that odor codes may support episodic memory in rodents (Manns et al. 2007) as well as social memory (Petrulis et al. 2005). Additionally, olfactospatial navigation in the absence of reliable allothetic or idiothetic cues, derived from other sensory modalities, supports the generation and stabilization of place fields (Zhang and Manahan-Vaughan 2015). Furthermore, the effectivity of odor-reward learning can be discriminated on the basis of neuronal oscillation patterns in the hippocampus (Rangel et al. 2016), indicating that odor processing is an intrinsic part of hippocampal information encoding.

The primary afferent input to the hippocampus comprises the perforant path that originates in the entorhinal cortex

(Andersen et al. 1971; Amaral and Witter 1989). The lateral entorhinal cortex receives sparse but nonetheless direct input from the lateral olfactory tract (Price 1973; Sosulski et al. 2011) and has strong connections with subcortical olfactory regions (Burwell and Amaral 1998; Kerr et al. 2007; Agster and Burwell 2009). One important route through which the olfactory bulb (OB) sends olfactory information to the olfactory system is via the lateral olfactory tract that projects to the piriform cortex, whereby a predominant portion of the tract terminates in the anterior piriform cortex (aPC) (Price 1973; Haberly 1985). The piriform cortex as a whole comprises the largest domain of the olfactory cortex and is particularly important for olfactory information processing because it is reciprocally connected to all parts of the entorhinal cortex, and especially with the lateral entorhinal cortex (Haberly and Price 1978; Burwell and Amaral 1998; Kerr et al. 2007; Agster and Burwell 2009). Whereas the medial entorhinal cortex is believed to serve as a spatial and visual processing domain and transfers associations from posterior brain regions to the hippocampus (Burwell 2000; Knierim et al. 2014; Witter et al. 2017), the lateral entorhinal cortex may convey unimodal sensory information and associations from more anterior brain regions, as well as attentional and motivational information aspects to the hippocampus (Burwell 2000; Knierim et al. 2014; Witter et al. 2017). The dentate gyrus (DG) appears to be exquisitely sensitive to olfactory experience: olfactory discrimination learning results in changes in evoked responses in the DG during and after learning (Chaillan et al. 1996; Chaillan et al. 1999; Truchet et al. 2002).

To what extent the potency of olfactory cues for both learning and memory retrieval relates to functional control by the olfactory cortex of the hippocampus is unknown. For this reason, in the present study, we set about to clarify 1) if stimulation of the aPC can evoke field potentials in the DG, 2) whether the aPC can trigger synaptic plasticity in the DG, 3) to what extent information transfer to the DG from the aPC is modulated by information transfer from the entorhinal cortex, and 4) where exactly in the DG information from the aPC is encoded. Our results provide the first evidence of specific control by the piriform cortex of hippocampal information encoding.

Materials and Methods

The study was carried out in accordance with the European Communities Council Directive of 22 September 2010 (2010/63/EU) for care of laboratory animals, and all experiments were conducted according to the guidelines of the German Animal Protection Law. They were approved in advance by the North Rhine-Westphalia (NRW) State Authority (Landesamt für Arbeitsschutz, Naturschutz, Umweltschutz und Verbraucherschutz, NRW). All efforts were made to reduce the number of animals used.

Surgery

Under sodium pentobarbital anesthesia (Nembutal, 52 mg/kg, intraperitoneal), male Wistar rats (9–10 weeks old, Charles River, Sulzfeld, Germany) were implanted chronically with electrodes (diameter: 0.1 mm, polyurethane-coated stainless-steel wire, Biomedical Instruments, Zöllnitz, Germany). Two screws served as reference or ground electrodes.

A monopolar recording electrode was positioned in the granule cell layer of the DG and a bipolar stimulation electrode in the perforant path (Fig. 1A), as described previously (Manahan–Vaughan and Reymann 1995). The final coordinates for the DG comprised −3.1 mm posterior to bregma (AP) and 1.9 mm lateral from midline (LAT) and for the perforant path: −6.9 mm AP and 4.1 mm LAT. The electrode positions and potentials evoked after recovery from surgery were consistent with a predominant stimulation of the medial perforant path (Manahan-Vaughan 2018).

In a second step, a bipolar electrode was implanted into the aPC. Depth profile responses (Manahan-Vaughan 2018) were obtained by recording from this electrode while stimulating the OB with a bipolar stimulation electrode (Fig. 1A). The coordinates used for the OB (+7.9 mm AP, 1.1–1.3 mm LAT) and aPC (+3.2–3.7 mm AP, 3.0–3.3 mm LAT) as described previously (Strauch and Manahan-Vaughan 2018) are based on coordinates used by Cohen and colleagues (Cohen et al., 2008). Following confirmation that the electrode was correctly placed in the aPC, this electrode was subsequently used as a stimulation electrode to evoke field potentials in the DG. To study the impact of the aPC on hippocampal information processing, stimulation was applied to the aPC only. Stimulation of the OB or the lateral olfactory tract would have complicated data interpretation, due to their additional activation of structures outside the aPC (Heimer 1968; Price 1973). For analgesia, animals were treated subcutaneously with Meloxicam (0.2 mg/kg; Metacam®, Boehringer Ingelheim Vetmedica GmbH, Ingelheim/Rhein, Germany), before and after surgery.

After recovery from surgery, animals were housed individually in a temperature- and humidity-controlled scantainer on a 12-h light/12-h dark cycle. They had ad libitum access to water and food.

Seven to 10 days after surgery, electrophysiological experiments were started, where the animals could move freely in a recording chamber ($40 \times 40 \times 50$ cm). Animals were connected via a flexible cable and a swivel connector to the stimulation unit (World Precision Instruments, Sarasota, FL, USA) and amplifier (A-M Systems, Sequim, WA, USA). Disturbance of the animals was kept to an absolute minimum, aside from the insertion of the connector cable at the start of each experiment.

Measurement of Evoked Potentials

Field excitatory postsynaptic potentials (fEPSPs) in the DG were generated by applying test-pulse stimulation in the aPC, or perforant path, at a low frequency with single biphasic square wave pulses of 0.2 ms duration per half wave. For each timepoint measured throughout the experiments, 5 evoked responses, (recorded every 60 s for aPC-DG and every 40 s for perforant path-DG), were averaged. The first 6 timepoints recorded at 5 min intervals were used as a baseline reference. All timepoints were calculated as a percentage of the mean of the 6 baseline timepoints. For the responses evoked in the DG by stimulating the aPC, the fEPSP was measured as the maximum amplitude from the onset of the fEPSP to the peak of the positive deflection of the evoked response. In perforant path–DG recordings, the population spike (PS) amplitude of the evoked responses was measured. An input/output (I/O) relationship (stimulus intensities from 100–900 µA applied in 100 µA steps) was used to determine the maximum fEPSP or PS. For the subsequent experiment, a stimulus intensity that produced 40–50% of the maximum response was chosen to evoke responses. Patterned afferent
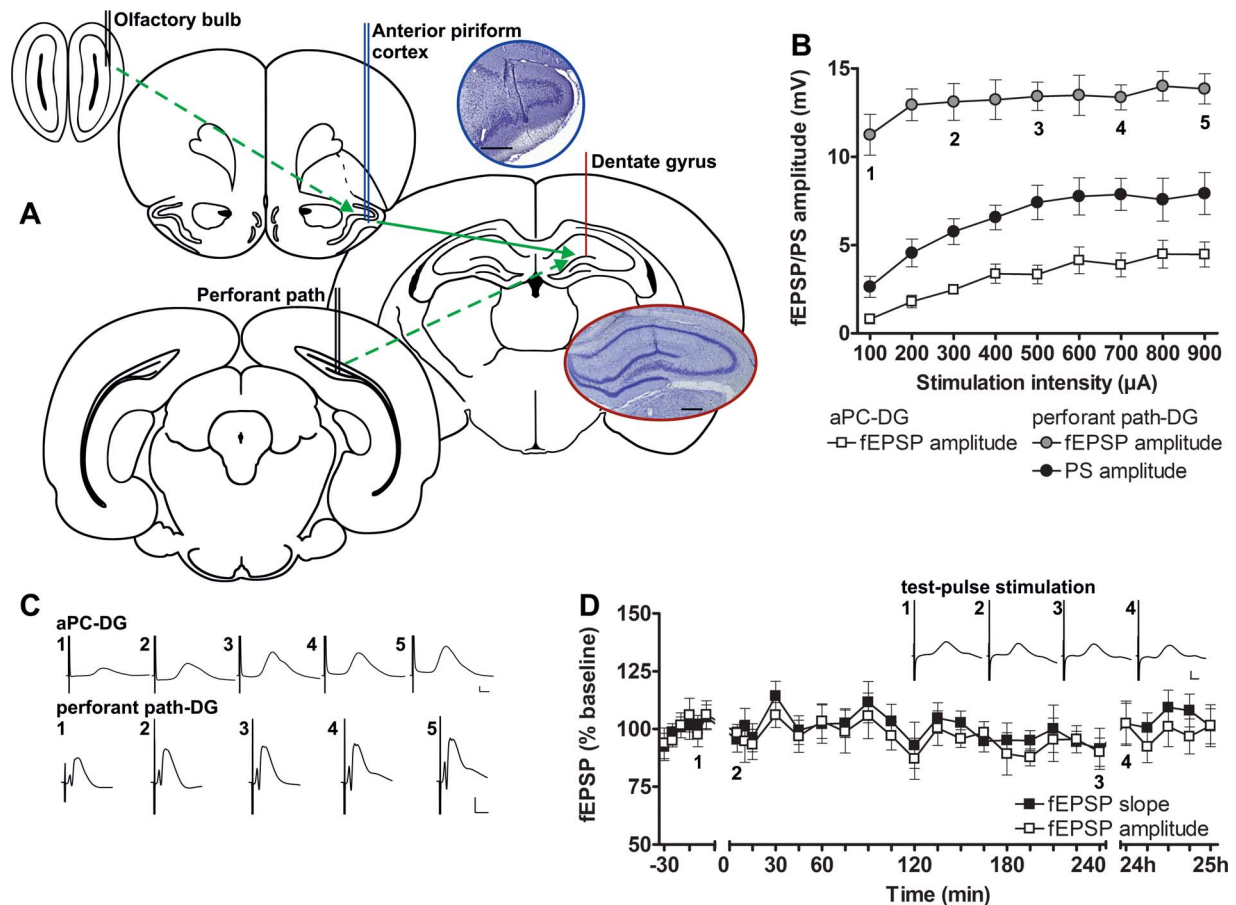
Figure 1. Electrode locations and comparison of electrophysiological responses evoked in the DG following aPC, or perforant path stimulation. (A) The recording electrode was positioned in the granule cell layer of the DG (red) by evoking potentials during depth profile recordings via a stimulation electrode placed in the perforant path (dashed green arrow). To ensure accurate placement of the electrode in the aPC (blue), it was first used to record responses during depth profile recordings via a stimulation electrode placed in the OB (dashed green arrow). The aPC electrode was subsequently used as a stimulation electrode, so that aPC–DG generated responses could be studied (solid green arrow). Coronal rat brain drawings, shown here, were modified from Paxinos and Watson (1998, 2005). Photomicrographs of Nissl-stained sections show placement of the stimulation electrode in the aPC (upper photo) and of the recording electrode in the DG (lower photo). Scale bars: 500 μm. (B) Input–output relationships for fEPSPs (aPC and DG) or PSs (DG only) were obtained using a stimulus intensity range of 100 to 900 μA for aPC–DG (squares, $n = 6$) and perforant path–DG (circles, $n = 5$). (C) Representative fEPSPs for both pathways evoked at increasing intensities: 1) 100 μA, 2) 300 μA, 3) 500 μA, 4) 700 μA, and 5) 900 μA. (D) Basal synaptic transmission of aPC–DG evoked responses remained stable with regard to both fEPSP amplitude and slope over a 24 h period ($n = 9$). Insets show representative fEPSPs evoked by test-pulse stimulation at the timepoints (1–4) indicated.
Calibration: Vertical bar: 1 mV, horizontal bar: 5 ms. *B, D* mean ± SEM.

stimulation was applied after the 30 min baseline recording. After 3 more recordings, at 5 min intervals, the interval was extended to 15 min. Evoked responses were followed for 4 h after application of patterned stimulation and on the following morning an additional hour of recordings (24 h recoding) was conducted. Only animals with stable test-pulse recordings over 4.5 h and during the 24 h recordings were used for experiments involving application of patterned stimulation. In experiments where patterned stimulation failed to induce synaptic plasticity, recordings were stopped 4 h after patterned stimulation. To avoid interaction effects of the different stimulation protocols, experiments were separated by intervals of at least 7 days.

Several protocols that are known to induce persistent synaptic plasticity in the hippocampal formation in freely behaving rats (Thiels et al. 1994; Manahan-Vaughan and Reymann 1995; Manahan-Vaughan 1997, 2000; Kemp and Manahan-Vaughan 2004, 2005) were applied to the aPC while recording in the DG. High-frequency stimulation (HFS) at 100 Hz was applied as 1 burst, or 4 bursts, of 100 pulses with an interburst interval of

5 min. Patterned stimulation at 30 Hz and 15 Hz was applied as 400 consecutive pulses. Low-frequency stimulation (LFS) at 1 Hz and 3 Hz was applied as 900 consecutive pulses at a stimulation intensity of 70% of the maximum evoked response during the I/O curve. Paired-pulse LFS consisted of 1800 pulses, given as 900 pairs at 1 Hz at 70% stimulation intensity (as determined by the I/O relationship) with an interpulse interval of 25 ms.

The effect of paired-pulse LFS of the aPC and/or the perforant path was compared. Therefore, in separate experiments, paired-pulse LFS was applied to either the aPC or the perforant path or to "both" (aPC and perforant path) simultaneously, and changes in either the aPC- or the perforant path–DG responses were examined.

In Situ Hybridization

Compartment analysis of temporal activity by fluorescence in situ hybridization (catFISH) was conducted using a modified procedure used by Guzowski and Worley (2001), as described

previously (Strauch and Manahan-Vaughan 2018). We exploited the fact that the peak somatic expression of the immediate early genes (IEGs), Homer1a and Arc, differ following a novel experience and used Homer1a expression to examine the effects of aPC stimulation on the DG, and Arc expression to study the effects of medial perforant path stimulation within the same animal. For Homer1a, somatic expression occurs approximately 25–40 min after commencement of a specific experience (Bottai et al. 2002; Vazdarjanova et al. 2002; Hoang et al. 2018), whereas for Arc, somatic expression occurs 2–15 min after an experience (Guzowski et al. 1999; Vazdarjanova et al. 2002; Hoang et al. 2018). After peak expression has occurred, the IEGs migrate to the cytoplasm (Guzowski et al. 1999; Guzowski et al. 2005). In the present study, brains were removed 40 min after commencement of LFS to the aPC. This meant that Homer1a could be used as a biomarker of somatic encoding caused by activation of the aPC. To use Arc as a biomarker for somatic encoding caused by perforant path stimulation, LFS of the perforant path was commenced in the same animal 10 min after conclusion of aPC stimulation.

Animals were implanted with electrodes as described above. On the experimental day, rats were first habituated to the recording chamber for approximately 1 h before LFS was applied. Paired pulse LFS (900 pulse pairs at 1 Hz) was applied at a stimulation intensity of 500 µA. To examine to what extent depolarization events (in the absence of induction of synaptic plasticity) result in IEG expression in the DG and to create a control condition against which LFS effects could be compared, a separate cohort of animals received test-pulse stimulation at 500 µA every 60 s for 15 min first in the aPC and after a break of 10 min in the perforant path. Brains were removed 40 min after the start of LFS, or of test-pulse stimulation in the aPC. They were then shock-frozen in 2-methylbutane at −80 to −100 °C on liquid nitrogen. Using a cryostat (Leica CM3050S), 20 µm thick coronal slices were sectioned. Sections of animals with incorrect electrode placement in the aPC or perforant path were excluded from further analysis.

Homer cDNA plasmids (Entelechon GmbH, Bad Abbach, Germany) with the sequence published by Brakeman et al. (1997) were linearized and an antisense RNA probe, labeled with biotin, was created (Ambion MaxiScript Kit, Invitrogen, Carlsbad, CA, USA). Arc cDNA plasmids (Entelechon GmbH) were generated using the sequence published by Lyford et al. (1995) and used to create digoxigenin-labeled RNA probes. Gel electrophoresis verified yield and integrity.

Slides containing the dorsal hippocampus (−3.6 to −4.0 mm posterior to Bregma) were fixed in 4% paraformaldehyde (PFA) solution, washed in 2× saline-sodium citrate buffer (SSC), placed in acetic anhydride solution, and washed and left in 2× SSC. In a humid chamber, slides were incubated with prehybridization buffer (Sigma-Aldrich, St. Louis, USA). Hybridization with biotin- and digoxigenin-labeled RNA probes (1 ng of each probe per µL) in hybridization buffer lasted overnight at 56 °C. Washing consisted of several steps in 2× SSC at 56 °C, 2× SSC containing RNase (1 µg/mL, Sigma-Aldrich) and 2× SSC at 37 °C, 0.5× SSC at 56 °C, and at RT, 1× SSC at RT and final rinsing in tris-buffered saline (TBS).

For Homer1a signal detection, slices were incubated for 70 min in 1% bovine serum-albumin (BSA) in TBS-Tween. Homer biotin was detected by Streptavidin CY2 (1:250, #016220084, Dianova, Hamburg, Germany) in 1% BSA in TBS-Tween for 30 min. Signal was enhanced with biotinylated Anti-Streptavidin (1:100, #BA0500, Vector Laboratories, Burlingame, CA, USA) in

1% BSA in TBS-Tween for 30 min. Homer1a was visualized by Streptavidin CY2 (1:250, Dianova). Arc signal detection consisted of H_2O_2 pretreatment, incubation in 1% BSA in TBS-Tween plus avidin (1:5; Avidin–biotin blocking kit, Vector Laboratories, Burlingame, CA, USA), detection by anti-digoxigenin-POD Fab fragment (1:400, #11207733910, Roche), enhancement using biotinylated tyramine (Adams 1992), and visualization with streptavidin Cy5 (1:2000, Dianova). Nuclei were visualized by 4′,6-diamidino-2-phenylindole (DAPI, 1:5000, Invitrogen). Finally, slides were mounted (SCR-38447, Dianova).

Homer1a and Arc mRNA expression within nuclei of granule cells in the DG was examined. Z-stacks were obtained using a fluorescence microscope (Zeiss ApoTome) that permits structured illumination microscopy (Schaefer et al. 2004), and was conducted at 63× magnification. For each region of each animal, 3 z-stacks from 3 consecutive sections were obtained. All z-stacks were chosen to contain representative regions of the upper and lower blade of the DG.

Postmortem Verification of Electrode Position

For verification of electrode position, brains were removed at the end of the study. The brain tissue was immediately fixed in 4% PFA solution in phosphate buffered saline (0.025 M, pH of 7.4) for 1 week. Then the tissue was cryoprotected by immersion in 30% sucrose for several days and 30 µm thick, frozen sections were cut on a freezing microtome (Leica Mikrosysteme Vertrieb GmbH, Wetzlar, Germany). Sections were mounted on glass slides and air-dried. Sections were stained in 0.1% cresyl violet (Mulisch and Welsch 2010; Hansen and Manahan–Vaughan 2015). Sections were examined using a microscope (Leica Mikrosysteme Vertrieb GmbH, Wetzlar, Germany) and photomicrographs (Fig. 1A) were taken with a digital video camera system (Visitron Systems, Germany). All animals with incorrect implanted electrodes were excluded from further analysis.

Data Analysis and Statistics

Data obtained in electrophysiological experiments were expressed as the mean percentage ± standard error of the mean (SEM) of the average baseline value. The results were visualized using GraphPad Prism software (GraphPad Software. Inc., La Jolla, CA, USA). To examine differences between basal synaptic transmission (test pulse only) and patterned stimulation, or to compare the effects of patterned stimulation in different brain regions, analysis of variance (ANOVA) with repeated measures was conducted using Statistica software (Version 12, StatSoft. Inc., Tulsa, OK, USA). To define onset and termination of synaptic plasticity, post-hoc Fisher's LSD tests were performed by determination of significances between the timepoints of the 2 test groups.

IEG expression in the DG was examined by marking complete nuclei and checking for Homer1a and Arc mRNA expression in each z-stack using ImageJ software. For each z-stack of the upper blade of the DG, 39 ± 2.27 cells were analyzed for the stimulated and 42 ± 1.92 cells for the control group and of the lower blade 48 ± 3.69 cells for the stimulated and 48 ± 2.05 cells for the control group were analyzed. During "experimenter-blind" analysis, the percentage of Homer1a and Arc positively stained nuclei of all nuclei was counted separately for each z-stack. Nuclei that were positive for both Arc and Homer1a mRNA were additionally assigned to a third group representing
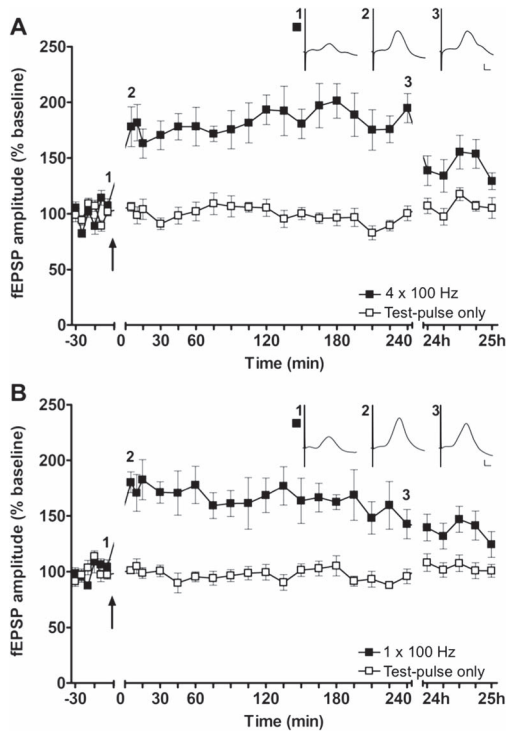
Figure 2. HFS applied to the aPC induces LTP in the hippocampus. HFS at 100 Hz induces LTP in the DG, when applied either as (A) 4 trains of 100 pulses or (B) 1 train of 100 pulses ($n = 10$) to the aPC. The arrow indicates the timepoint at which HFS was applied. Insets show analog examples of fEPSPs evoked prior to (1), 5 min after (2), and 4 h after (3) HFS.
Calibration: Vertical bar: 1 mV, horizontal bar: 5 ms. A–C mean ± SEM.

cells that were active during LFS of the aPC, as well as in the perforant path. The mean of 3 z-stacks was calculated for each animal and the mean percentage ± SEM was visualized using GraphPad. For statistical analysis of IEG expression, unpaired Student's t-tests were performed to examine difference between LFS and test-pulse stimulation.

The level of significance was set to $P < 0.05$. The sample size n corresponds to the number of individual animals.

Results

Test-Pulse Stimulation of the aPC Evokes Local Field Potentials in the DG

We applied test pulses to the aPC in the range of 100 to 900 μA to clarify to what extent local field potentials can be directly evoked in the DG by aPC activity ($n = 6$, Fig. 1B). We observed field potentials, the onset of which typically began approximately 10 ms after the stimulus artifact (Fig. 1C), compared with 1–2 ms for potentials that were evoked by perforant path stimulation (Fig. 1C). The frequency–amplitude relationship of aPC–DG potentials was lower than those evoked by direct perforant path stimulation ($n = 5$, Fig. 1B). Field potentials were typically smaller and lacked a PS compared with perforant path–DG evoked potentials (Fig. 1B). Nonetheless, field potentials evoked by test-pulse stimulation of the aPC were stable across a 24 h period ($n = 9$, Fig. 1D).

HFS of the aPC Induces Long-Term Potentiation in the DG, whereas LFS Induces Short-Term Depression

We then evaluated whether patterned stimulation of the aPC results in synaptic plasticity in the DG. We observed that HFS as 4 bursts of 100 pulses results in long-term potentiation (LTP) that lasts for over 24 h ($n = 10$, Fig. 2A, Table 1). Reducing the number of bursts to one ($n = 10$) did not alter the outcome: LTP (>24 h) was also induced in this case (Fig. 2B, Table 1).

Having observed LTP following HFS of the aPC, we went on to explore whether lower stimulation frequencies have an impact on plasticity responses in the DG. Here we found that 30-Hz (given as 400 pulses) ($n = 8$, Fig. 3A) or 15 Hz stimulation (400 pulses) ($n = 8$, Fig. 3B) that reflect the range of olfactory beta frequency oscillatory activity (Kay et al. 2009), both resulted in a modest slow-onset potentiation in the DG (Table 1). By contrast, neither 3 Hz ($n = 9$, Fig. 3C) nor 1 Hz ($n = 8$, Fig. 3D) stimulation (both given as 900 consecutive pulses) resulted in any change of synaptic strength (Table 1).

To examine if a stronger and more physiological LFS protocol elicits synaptic plasticity (Thiels et al. 1994; Thiels et al. 1996), we tested paired-pulse LFS. This protocol comprised applying 900 pulse pairs (interpulse interval of 25 ms) at 1 Hz ($n = 9$). Here, LFS resulted in short-term depression (STD) that lasted for 1 to 1.5 h (Fig. 3E, Table 1).

Synaptic Plasticity Triggered by Perforant Path Stimulation Overrides Piriform Cortex–DG Plasticity

Having observed that the aPC can directly trigger various kinds of hippocampal plasticity, we explored whether medial perforant path–DG plasticity and aPC–DG plasticity synergize in any way. It is well known that patterned stimulation of the perforant path results in both LTP (>24 h) (Manahan-Vaughan and Reymann 1995; Klausnitzer et al. 2004; Manahan-Vaughan and Schwegler 2011; Kenney and Manahan-Vaughan 2013) and

Table 1 Overview of stimulation protocols used to stimulate the aPC and the outcome of statistical analysis for the aPC–DG responses

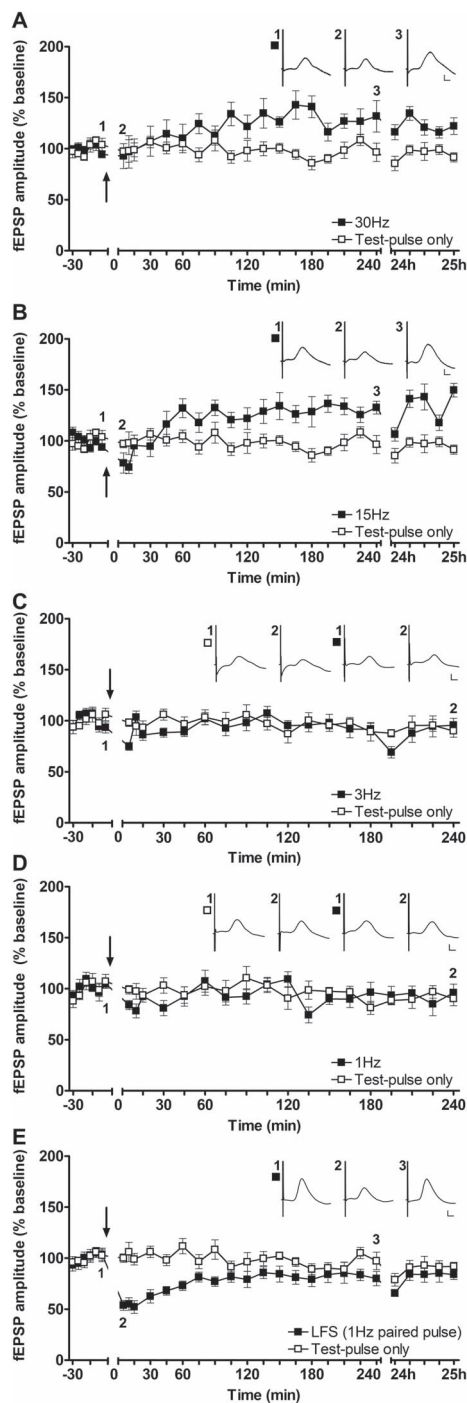|	n	ANOVA: fEPSP amplitude
100 Hz 4 bursts of 100 pulses	10	$F_{(1,18)} = 66.411$, **$P < 0.000001$**
100 Hz 1 burst of 100 pulses	10	$F_{(1,18)} = 27.737$, **$P < 0.0001$**
30 Hz 400 pulses	8	$F_{(1,14)} = 11.166$, **$P < 0.01$**
15 Hz 400 pulses	8	$F_{(1,14)} = 26.867$, **$P < 0.001$**
3 Hz 900 pulses 70% (4 h)	9	$F_{(1,16)} = 1.83$, $P = 0.195$
1 Hz 900 pulses 70% (4 h)	8	$F_{(1,14)} = 0.895$, $P = 0.36$
1 Hz 900 paired pulses 25-ms interval 70%	9	$F_{(1,16)} = 26.236$, **$P < 0.001$**

Figure 3. Patterned stimulation of the aPC in the frequency range of beta oscillations, as well as paired-pulse LFS, induces synaptic plasticity in the hippocampus. (A,B) Stimulation of the aPC at 30 Hz (A, $n = 8$) or 15 Hz (B, $n = 8$) results in slow-onset potentiation in the DG of behaving rats. Insets show representative fEPSPs evoked prior to (1), 5 min following (2), and 4 h after (3) patterned stimulation. (C–D) Stimulation (C) at 3 Hz ($n = 9$) or (D) at 1 Hz ($n = 8$) of the aPC fails to change synaptic transmission in the DG. Insets: Representative fEPSPs evoked prior to (1) and 4 h after (2) test-pulse stimulation (left set of analogs) or patterned stimulation (right set of analogs). (E) Paired-pulse LFS (1 Hz, 900 pulse pairs) of the aPC induces STD in the DG ($n = 9$). Insets: Analog examples of fEPSPs evoked at the timepoints indicated either prior to (1) or after (2, 3) LFS. Calibration: Vertical bar: 1 mV, horizontal bar: 5 ms. A–E mean ± SEM. The arrow in each graph indicates the timepoint at which patterned stimulation was applied.

long-term depression (LTD, >24 h) (Klausnitzer et al. 2004; Manahan-Vaughan and Schwegler 2011; Kenney and Manahan–Vaughan 2013; Wieschelleck and Manahan-Vaughan 2014) in the DG of freely behaving rats.

We compared DG field potentials that were evoked by aPC stimulation after the following 3 treatments (all involving paired pulse LFS (1 Hz, 900 pulse pairs)):

1. LFS applied to the aPC "only" ($n = 6$).
2. LFS applied to the medial perforant path "only" ($n = 6$).
3. LFS applied to the aPC and the medial perforant path "simultaneously" ($n = 6$).

LFS of the medial perforant path elicited a modest and transient slow-onset potentiation of aPC–DG synaptic responses, whereas LFS given to the aPC resulted in STD of aPC–DG responses (Fig. 4A, Table 2). Simultaneous application of LFS to both inputs resulted in inhibition of aPC–DG STD, and evoked responses were not significantly different from those elicited after LFS to the perforant path alone (Fig. 4A, Table 2).

We then compared DG field potentials elicited by test pulses given to the medial perforant path following the same 3 treatments listed above (all $n = 7$): LFS of the perforant path alone resulted in LTD of perforant path–DG synapses, whereas LFS given to the aPC resulted in slow-onset depression of perforant path–DG synapses (Fig. 4B, Table 3). Simultaneous application of LFS to both inputs resulted in LTD of perforant path–DG synapses that was not significantly different from LTD elicited by perforant path–DG stimulation alone (Fig. 4B, Table 3).

Taken together, these results show that synaptic plasticity elicited in aPC–DG responses is distinct from plasticity evoked in medial perforant path–DG responses, despite the fact that the aPC is connected to both the medial and lateral entorhinal cortex (Burwell and Amaral 1998; Kerr et al. 2007) and the afferent route to the DG from both structures is the perforant path. One possible explanation for this effect is that information from the aPC may be brought to the hippocampus by the "lateral" perforant path, consistent with the stronger connection of the aPC to the lateral entorhinal cortex (Haberly and Price 1978; Burwell and Amaral 1998; Kerr et al. 2007).

Induction of Hippocampal Synaptic Plasticity by Stimulation of the Piriform Cortex Is Associated With Somatic Information Encoding

We then explored to what extent activation of the aPC and the medial perforant path is associated with the expression of the IEGs Homer1a and Arc in the DG granule cells, which function as indicators of neuronal activity and experience-dependent information encoding (Guzowski et al. 1999; Bottai et al. 2002; Vazdarjanova et al. 2002; Hoang et al. 2018). Each animal received LFS (900 pulse pairs at 1 Hz) of the aPC followed by LFS of the perforant path. The timing of these events was planned so that somatic Homer1a expression in the DG reflected aPC stimulation and Arc expression in the DG reflected the effects of medial perforant path stimulation. We discriminated between the upper and lower blades of the DG, given our previous findings that these structures process "what" (upper blade) and "where" (lower blade) information differently (Hoang et al., 2018) and given reports that the lateral and medial perforant paths may project in a differentiated manner to these structures (Wyss 1981; Tamamaki 1997).
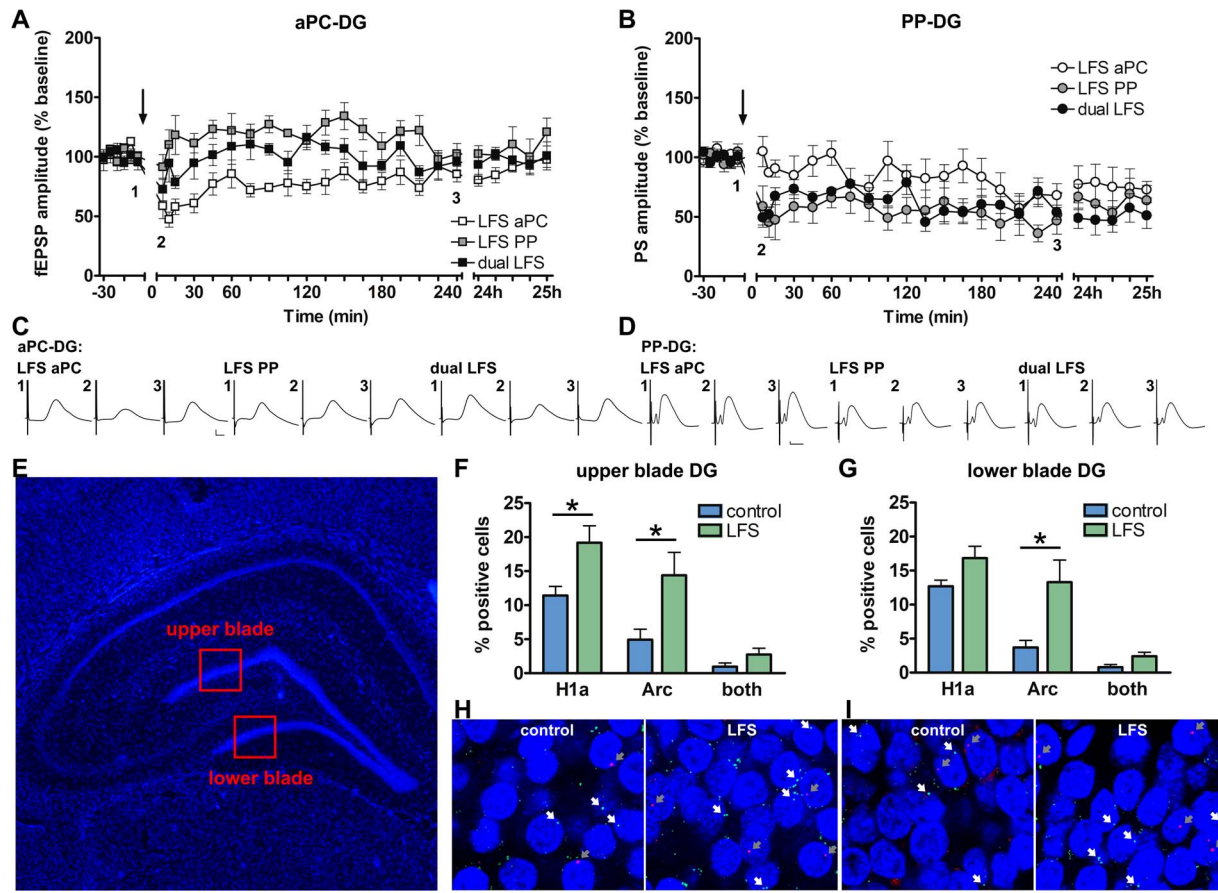
Figure 4. Stimulation of the perforant path (PP) overrides plasticity induced by piriform cortex activation. Induction of hippocampal synaptic plasticity by stimulation of the aPC or PP results in an increase of IEG expression in the DG. (A) Potentials were evoked in the DG by stimulating the aPC. LFS (1 Hz, 900 pulse pairs) of the aPC results in synaptic depression of aPC–DG responses. LFS of the PP results in a modest, slow-onset potentiation of aPC–DG responses. "Simultaneous" LFS of both the PP ($n = 6$) and aPC ($n = 6$) results in the predomination of the PP-mediated plasticity response at aPC–DG responses: a synaptic response resulted that was not significantly different from aPC–DG responses triggered by LFS of the PP "alone". (B) Potentials were evoked in the DG by stimulating the PP. LFS of the aPC and/or PP results in synaptic depression in the PP-DG synapses ($n = 7$, each). The arrow indicates the timepoint at which LFS was applied. (C–D) Representative fEPSPs evoked prior to (1), 5 min after (2), and 4 h after LFS (3). Calibration: Vertical bar: 1 mV, horizontal bar: 5 ms. (E) 4',6-diamidino-2-phenylindole (DAPI)-stained section of the rat hippocampus showing the dorsal DG regions that were analyzed in the IEG study (red squares). (F) The IEGs, Arc, and Homer1a were examined in the brains of animals that received consecutive LFS of the aPC and PP, or received test-pulse stimulation under the same test conditions (controls). Somatic Homer1a expression reflects aPC stimulation and somatic Arc expression reflects PP stimulation. IEG expression in the upper blade of the DG is significantly increased after LFS of either the aPC (Homer1a) or the PP (Arc), compared with test-pulse stimulated controls ($n = 6$, each). (G) LFS of the aPC does not significantly alter Homer1a expression in the lower blade of the DG, whereas Arc mRNA levels increase in this region after LFS of the PP (compared with controls, all $n = 6$). (H–I) Photomicrographs of (H) the upper blade and (I) the lower blade of the DG showing Homer1a mRNA (green), Arc mRNA (red), and DAPI-stained nuclei of DG granule cells (blue) following LFS or test-pulse stimulation (controls). Homer1a mRNA positive nuclei are indicated by a white arrow and Arc mRNA positive nuclei are indicated by a gray arrow. Images were taken using a 63× objective. A–B, F–G mean ± SEM. F–G ∗ = significance.

Somatic Homer1a mRNA expression was significantly increased in the upper blade of the DG after aPC stimulation compared with controls ($n = 6$, Fig. 4F, Table 4). In contrast, effects were not significant in the lower blade, although a slight increase was evident ($n = 6$, Fig. 4G, Table 4). These results are consistent with aPC inputs to the DG being mediated by the lateral perforant path that has been proposed to project predominantly to the upper blade of the DG (Wyss 1981; Tamamaki 1997).

Following LFS of the medial perforant path, Arc mRNA levels increased in somata of both blades of the DG compared with test-pulse stimulated controls ($n = 6$, each; Fig. 4F–I; Table 4).

The number of somata that expressed both Arc and Homer1a was low and not significant compared with test-pulse controls (Fig. 4F–I, Table 4), suggesting that aPC and medial perforant path stimulation targeted different populations of DG cells, con-sistent with a possible transmission of aPC information to the DG via the lateral perforant path.

Discussion

This study provides the first evidence that activity in the piri-form cortex evokes field potentials in the DG and can also trigger frequency-dependent forms of synaptic plasticity. Effects are associated with the expression of the IEG, Homer1a, in granule cells of the DG, indicating that experience-dependent infor-mation processing is enabled by piriform cortex activity. The profile of synaptic plasticity induced by aPC activation is dis-tinct to plasticity that is triggered by perforant path activation, suggesting that the piriform cortex can influence hippocampal information encoding in defined and distinct ways.

Table 2 Overview of the outcome of statistical analysis for paired-pulse LFS (1 Hz, 900 pulse pairs) in the aPC (aPC) and/or the perforant path for the aPC–DG responses

LFS: aPC–DG ($n = 6$)	ANOVA: fEPSP amplitude
Test pulse vs. LFS perforant path	$F_{(1,10)} = 5.112$, **$P < 0.05$**
Test pulse vs. LFS aPC	$F_{(1,10)} = 21.151$, **$P < 0.001$**
Test pulse vs. dual LFS	$F_{(1,10)} = 0.202$, $P = 0.663$
LFS perforant path vs. LFS aPC	$F_{(1,10)} = 25.2753$, **$P < 0.001$**
LFS perforant path vs. dual LFS	$F_{(1,10)} = 4.2052$, $P = 0.067$
LFS aPC vs. dual LFS	$F_{(1,10)} = 7.5544$, **$P < 0.05$**

Table 3 Overview of the outcome of statistical analysis for paired-pulse LFS (1 Hz, 900 pulse pairs) in the aPC (aPC) and/or the perforant path for the perforant path–DG responses

LFS: perforant path–DG ($n = 7$)	ANOVA: PS amplitude
Test pulse vs. LFS perforant path	$F_{(1,12)} = 23.9552$, **$P < 0.001$**
Test pulse vs. LFS aPC	$F_{(1,12)} = 4.5817$, $P = 0.054$
Test pulse vs. dual LFS	$F_{(1,12)} = 69.149$, **$P < 0.00001$**
LFS perforant path vs. LFS aPC	$F_{(1,12)} = 7.5084$, **$P < 0.05$**
LFS perforant path vs. dual LFS	$F_{(1,12)} = 0.2134$, $P = 0.652$
LFS aPC vs. dual LFS	$F_{(1,12)} = 11.0755$, **$P < 0.01$**

Table 4 Outcome of statistical analysis (*t*-tests) of the expression of Homer 1a RNA, Arc mRNA, and double-labeled nuclei in the upper and lower blade of the DG after LFS (1 Hz 900 pulse airs) of the aPC (Homer1a) and perforant path (Arc) compared with test-pulse stimulated controls

$n = 6$ per group	Upper blade	Lower blade
Homer1a mRNA	$t_{(10)} = 2.494$, **$P < 0.05$**	$t_{(10)} = 1.926$, $P = 0.083$
Arc mRNA	$t_{(10)} = 2.323$, **$P < 0.05$**	$t_{(10)} = 2.573$, **$P < 0.05$**
Double labelling	$t_{(10)} = 1.495$, $P = 0.166$	$t_{(10)} = 2.045$, $P = 0.068$

Our observation that direct stimulation of the aPC triggers synaptic plasticity in the DG was quite surprising. Although the visual system can be assumed to be a major determinant of experience encoding in the hippocampus, stimulation of the visual cortex does not evoke field potentials or directly trigger synaptic plasticity in the DG, although it does alter excitability and neuronal oscillations there (Tsanov and Manahan-Vaughan 2009). Until now, only one other study addressed whether the piriform cortex can influence hippocampal synaptic encoding: Racine et al. (1983) provided early evidence that the piriform cortex influences synaptic plasticity in the DG. They showed that repetitive HFS of the piriform cortex at 400 Hz, in a kindling-like paradigm, applied over several days elicits weak synaptic potentiation in the DG in vivo (Racine et al. 1983).

We observed that a "single" 100 pulse train of 100 Hz stimulation of the aPC results in persistent LTP in the DG. This is a very striking effect, given that the same protocol, when applied of the perforant path, triggers at most, short-term potentiation in perforant path–DG synapses (Kenney and Manahan-Vaughan 2013). This suggests that activity in the aPC is readily capable of triggering long-term information storage in the hippocampus.

In addition to the induction of LTP and synaptic depression, in aPC–DG responses, we observed a modest slow-onset potentiation that resulted from stimulation at 15 or 30 Hz. Both protocols are in the range of beta oscillatory activity (15–40 Hz) that is known to occur during odorant presentation and during olfactory association learning in parts of the olfactory system, such as the OB, piriform cortex, and entorhinal cortex (Boeijinga and Lopes Da Silva 1989; Chapman et al. 1998; Ravel et al. 2003; Martin et al. 2004; Martin et al. 2007; Chapuis et al. 2009; Kay and Beshel 2010). These frequencies also occur in associated brain regions such as the orbitofrontal cortex, amygdala, and the hippocampal formation (Vanderwolf 1992; Heale et al. 1994; Chapman et al. 1998; Ravel et al. 2003; Martin et al. 2007; Chapuis et al. 2009). Two studies mimicked olfaction-induced beta oscillations in the DG by applying patterned stimulation to the OB or posterior piriform cortex (pPC) (Heale and Vanderwolf 1995; Chapman et al. 1998), suggesting that patterned stimulation at 15 or 30 Hz may serve to mimic effects of odor presentation and emulate beta oscillations in the aPC. It was also suggested that neuronal activity in the beta frequency range might play a role in gating of sensory input to the hippocampal formation (Chapman et al. 1998). Our data indicate that this process may be reflected by the occurrence of slow-onset potentiation in the DG.

Olfactory information from the piriform cortex is relayed via the entorhinal cortex to the hippocampus (Cragg 1960; Price 1973; Beckstead 1978; Burwell and Amaral 1998; Kerr et al. 2007; Ohara et al. 2013). The entorhinal cortex projects to the hippocampus via the perforant path. We observed that under circumstances where the medial perforant path was stimulated, synaptic plasticity triggered by aPC stimulation was subordinate to hippocampal instruction by the entorhinal cortex. Three possible interpretations of this effect spring to mind:

1. The synaptic plasticity elicited by the aPC still occurred within DG synapses, but detection was occluded by the induction of medial perforant path–DG plasticity.

2. Activity in aPC was transmitted to the DG via the lateral perforant path, whereas our direct perforant path stimulation targeted mainly the medial path.

3. aPC–DG plasticity is vetoed by conjunctive (or additional) activity in the entorhinal cortex. One could envisage that this might occur under circumstances where another sensory modality might be deemed more salient or reliable in terms of information encoding.

Indeed, we have observed a hierarchy of this kind with regard to hippocampal LTD that is enabled by sensory spatial learning. In the CA1 region of freely behaving rats, visuospatial learning (Manahan-Vaughan and Braunewell 1999; Kemp and Manahan-Vaughan 2004), olfactospatial learning (André and Manahan-Vaughan 2013), and audiospatial learning (Dietz and Manahan-Vaughan 2017) all facilitate the expression of LTD. Here, in terms of the magnitude and persistence of the resultant LTD, a hierarchy is apparent whereby visuospatial learning-related LTD > olfactospatial learning LTD > audiospatial learning LTD. A similar pattern emerges when one compares place fields that emerge as a result of spatial sensory navigation. Here, when rats explore space in the absence of reliable cues from any other sensory modality, place field precision and stability is higher when visuospatial cues are explored compared with olfactospatial cues (Zhang and Manahan-Vaughan 2015).

Both lateral and medial entorhinal cortices have reciprocal connections with the piriform cortex, whereby more connections are made with the lateral part (Burwell and Amaral 1998; Kerr et al. 2007; Agster and Burwell 2009). Thus, most olfactory sensory information is projected via the lateral entorhinal cortex to the hippocampal formation (Beckstead 1978; Burwell and Amaral 1998; Kerr et al. 2007), probably via a distinct cell population in layer II that is projecting to the DG (Leitner et al. 2016). The lateral entorhinal cortex is believed to convey unimodal sensory information, attentional and motivational information aspects to the hippocampus as well as polymodal associations from anterior brain regions, such as medial and orbital frontal regions (Burwell 2000; Knierim et al. 2014; Witter et al. 2017). Whereas the lateral entorhinal cortex conveys less information about space (Hargreaves et al. 2005), its activity is more related to an item's, or cue's, features (so-called "what" information), such as specific odors (Deshmukh and Knierim 2011; Knierim et al. 2014; Li et al. 2017). By contrast, the medial entorhinal cortex conveys information about spatial characteristics ("where" information) (Witter et al. 2000; Henriksen et al. 2010; Burke et al. 2011; Sauvage et al. 2013). The distinct synaptic plasticity profiles, as well as the nearly nonoverlapping increase in Homer1a and Arc mRNA expression induced by either LFS of the aPC, or perforant path, is likely to reflect activation of the lateral entorhinal cortex by aPC stimulation. By contrast, the profiles of the fEPSPs elicited in the DG via perforant path stimulation suggest that the medial perforant path was mainly activated (Manahan-Vaughan 2018).

The impact of medial versus lateral perforant path stimulation on the DG is well described (Abraham et al. 1985; Colino and Malenka 1993; Abraham et al. 1994; Abraham et al. 2006). Homosynaptic LTP in the DG can be induced by stimulation of either the lateral or the medial perforant path and is accompanied by heterosynaptic synaptic depression in the other pathway (Abraham et al. 1985; Abraham et al. 1994). LTP in the DG is stronger after induction in the medial compared with the lateral perforant path. Moreover, heterosynaptic depression in the medial perforant path–DG synapses induced by lateral per-

forant path stimulation is weaker than heterosynaptic depression induced in the lateral perforant path–DG synapses induced by medial perforant path stimulation (Abraham et al. 1985; Abraham et al. 1994). This suggests that the medial perforant path may be the dominant information source for the hippocampus under conditions where both paths compete.

In line with this interpretation and the above-mentioned possibility that the aPC transmits its information to the DG via the lateral perforant path, we detected a significant increase in the number of granule cells that expressed Homer1a in the upper blade of the DG following patterned stimulation of the aPC, whereas patterned stimulation of the perforant path resulted in an increase in Arc expression in both upper and lower blade of the DG. Anatomical studies have indicated that the lateral entorhinal cortex projects primarily to the upper blade and that the medial entorhinal cortex projects primarily to the lower blade of the DG (Wyss 1981; Tamamaki 1997). Thus, aPC activation probably changed neuronal activity in the lateral entorhinal cortex that in turn was conveyed to the DG, whereas medial perforant path activation emulated activation of the medial entorhinal cortex.

Information encoded by the DG may take the form of "discrete" directional cues (e.g., visible landmarks) or "distributed" directional cues such as odor gradients (Jacobs 2012; Jacobs and Menzel 2014). We have proposed that the upper blade of the DG preferentially processes "what" information, whereas the lower blade of the DG processes "where" information (Hoang et al. 2018). More specifically, a differentiation may be enabled by the DG whereby "distributed" directional cue (e.g., "what") information is preferentially encoded by the upper blade, and "discrete" directional cue (e.g., "where") information is encoded by the lower blade (Hoang et al. 2018). Interpreted from this basis, our current results suggest that the information relayed by the piriform cortex to the hippocampus for DG encoding relates to odor identity and possibly to odor context.

In line with this possibility, a very close association between odor identification and spatial memory ability in humans was recently reported (Dahmani et al. 2018). Odors can support orientation in a room with no other sensory cues available (Jacobs et al. 2015) and associative olfactory learning can influence synaptic transmission and excitability in the rodent hippocampal formation (Chaillan et al. 1996; Chaillan et al. 1999; Mouly et al. 2001; Truchet et al. 2002; Zelcer et al. 2006). Furthermore, novel odor-place experience facilitates the expression of hippocampal LTD in rodents (André and Manahan-Vaughan 2013) and recently it was reported that the lateral entorhinal cortex–CA1 pathway is critically involved in olfactory associative learning (Li et al. 2017). This latter effect may be mediated via the posterior piriform cortex (pPC) that has been proposed to engage in dynamic categorization of the quality and similarity of learned odors (Kadohisa and Wilson 2006; Howard et al. 2009; Gottfried 2010). By contrast, the human and also the rodent aPC has been proposed to support the determination of odor identity (Gottfried et al. 2006; Kadohisa and Wilson 2006; Gottfried 2010). Taken together with previous observations as to the relationship between learning olfactospatial relationships and the induction of hippocampal synaptic plasticity (André and Manahan-Vaughan 2013), our data suggest that in rodents, the aPC may serve to identify odor objects that can be used for spatial encoding by the hippocampus. The pPC, by contrast, may support multisensory encoding (Li et al. 2017). Here, one could speculate that a differentiation between aPC-mediated "simple" odor encoding

in the upper blade of the DG and pPC-mediated higher order odor encoding in the cornus ammonis may occur (Li et al. 2017).

Our results suggest that information from the aPC is likely to reach the DG via the lateral perforant path and, strikingly, in a competitive situation, encoding of information that is transmitted by the medial perforant path predominates above aPC-mediated information. Little is known about how olfaction and vision are integrated and calibrated in the context of multisensory spatial orientation by the hippocampus. The role of the entorhinal cortex in gating inputs or weighting different sensory modalities is also unclear. Our observation that direct medial perforant path stimulation can subordinate hippocampal information encoding by the aPC suggests that cue competition may occur at the level of sensory inputs that are gated by the lateral and entorhinal cortices.

Conclusions

In this study, we provide the first evidence that hippocampal synaptic plasticity, in the forms of LTP and LTD, can be directly induced by patterned stimulation of the aPC. Identical stimulation protocols, given either directly to the medial perforant path, or to the aPC, resulted in different patterns of somatic IEG expression in the DG and also resulted in different profiles of synaptic plasticity in the DG.

Our results support that the piriform cortex engages in specific control of hippocampal information processing and encoding that may serve as a functional mechanism for the integration of olfactory experience into hippocampal representations and associative memory. This study, thus, provides a critical foundation for our understanding of how the olfactory system drives information encoding in the hippocampal formation.

Funding

Notes

Author contributions

The study was designed by D.M.-V. Experiments were conducted by C.S. and analyzed by both authors. D.M.-V. wrote the paper, together with C.S.

References

Abraham WC, Bliss TV, Goddard GV. 1985. Heterosynaptic changes accompany long-term but not short-term potentiation of the perforant path in the anaesthetized rat. *J Physiol*. 363:335–349.

Abraham WC, Christie BR, Logan B, Lawlor P, Dragunow M. 1994. Immediate early gene expression associated with the persistence of heterosynaptic long-term depression in the hippocampus. *Proc Natl Acad Sci U S A*. 91:10049–10053.

Abraham WC, Mason-Parker SE, Irvine GI, Logan B, Gill AI. 2006. Induction and activity-dependent reversal of persistent LTP and LTD in lateral perforant path synapses in vivo. *Neurobiol Learn Mem*. 86:82–90.

Adams JC. 1992. Biotin amplification of biotin and horseradish peroxidase signals in histochemical stains. *J Histochem Cytochem*. 40:1457–1463.

Agster KL, Burwell RD. 2009. Cortical efferents of the perirhinal, postrhinal, and entorhinal cortices of the rat. *Hippocampus*. 19:1159–1186.

Amaral DG, Witter MP. 1989. The three-dimensional organization of the hippocampal formation: a review of anatomical data. *Neuroscience*. 31:571–591.

Andersen P, Bliss TV, Skrede KK. 1971. Unit analysis of hippocampal polulation spikes. *Exp Brain Res*. 13:208–221.

André MA, Manahan-Vaughan D. 2013. Spatial olfactory learning facilitates long-term depression in the hippocampus. *Hippocampus*. 23:963–968.

Beckstead RM. 1978. Afferent connections of the entorhinal area in the rat as demonstrated by retrograde cell-labeling with horseradish peroxidase. *Brain Res*. 152:249–264.

Bird CM, Burgess N. 2008. The hippocampus and memory: insights from spatial processing. *Nat Rev Neurosci*. 9:182–194.

Boeijinga PH, Lopes da Silva FH. 1989. Modulations of EEG activity in the entorhinal cortex and forebrain olfactory areas during odour sampling. *Brain Res*. 478:257–268.

Bottai D, Guzowski JF, Schwarz MK, Kang SH, Xiao B, Lanahan A, Worley PF, Seeburg PH. 2002. Synaptic activity-induced conversion of intronic to exonic sequence in Homer 1 immediate early gene expression. *J Neurosci*. 22:167–175.

Brakeman PR, Lanahan AA, O'Brien R, Roche K, Barnes CA, Huganir RL, Worley PF. 1997. Homer: a protein that selectively binds metabotropic glutamate receptors. *Nature*. 386:284–288.

Burke SN, Maurer AP, Nematollahi S, Uprety AR, Wallace JL, Barnes CA. 2011. The influence of objects on place field expression and size in distal hippocampal CA1. *Hippocampus*. 21:783–801.

Burwell RD. 2000. The parahippocampal region: corticocortical connectivity. *Ann N Y Acad Sci*. 911:25–42.

Burwell RD, Amaral DG. 1998. Cortical afferents of the perirhinal, postrhinal, and entorhinal cortices of the rat. *J Comp Neurol*. 398:179–205.

Chaillan FA, Roman FS, Soumireu-Mourat B. 1996. Modulation of synaptic plasticity in the hippocampus and piriform cortex by physiologically meaningful olfactory cues in an olfactory association task. *J Physiol Paris*. 90:343–347.

Chaillan FA, Truchet B, Roman FS, Soumireu-Mourat B. 1999. Early polysynaptic potentiation recorded in the dentate gyrus during an associative learning task. *Neuroscience*. 94:443–451.

Chapman CA, Xu Y, Haykin S, Racine RJ. 1998. Beta-frequency (15–35 Hz) electroencephalogram activities elicited by toluene and electrical stimulation in the behaving rat. *Neuroscience*. 86:1307–1319.

Chapuis J, Garcia S, Messaoudi B, Thevenet M, Ferreira G, Gervais R, Ravel N. 2009. The way an odor is experienced during aversive conditioning determines the extent of the network recruited during retrieval: a multisite electrophysiological study in rats. *J Neurosci*. 29:10287–10298.

Cohen Y, Reuveni I, Barkai E, Maroun M. 2008. Olfactory learning-induced long-lasting enhancement of descending

and ascending synaptic transmission to the piriform cortex. *J Neurosci*. 28:6664–6669.

Colino A, Malenka RC. 1993. Mechanisms underlying induction of long-term potentiation in rat medial and lateral perforant paths in vitro. *J Neurophysiol*. 69:1150–1159.

Cragg BG. 1960. Responses of the hippocampus to stimulation of the olfactory bulb and of various afferent nerves in five mammals. *Exp Neurol*. 2:547–572.

Dahmani L, Patel RM, Yang Y, Chakravarty MM, Fellows LK, Bohbot VD. 2018. An intrinsic association between olfactory identification and spatial memory in humans. *Nat Commun*. 9:4162.

Deshmukh SS, Knierim JJ. 2011. Representation of non-spatial and spatial information in the lateral entorhinal cortex. *Front Behav Neurosci*. 5:69.

Dietz B, Manahan-Vaughan D. 2017. Hippocampal long-term depression is facilitated by the acquisition and updating of memory of spatial auditory content and requires mGlu5 activation. *Neuropharmacology*. 115:30–41.

Eichenbaum H, Robitsek RJ. 2009. Olfactory memory: a bridge between humans and animals in models of cognitive aging. *Ann N Y Acad Sci*. 1170:658–663.

Gottfried JA. 2010. Central mechanisms of odour object perception. *Nat Rev Neurosci*. 11:628–641.

Gottfried JA, Winston JS, Dolan RJ. 2006. Dissociable codes of odor quality and odorant structure in human piriform cortex. *Neuron*. 49:467–479.

Guzowski JF, McNaughton BL, Barnes CA, Worley PF. 1999. Environment-specific expression of the immediate-early gene arc in hippocampal neuronal ensembles. *Nat Neurosci*. 2:1120–1124.

Guzowski JF, Timlin JA, Roysam B, McNaughton BL, Worley PF, Barnes CA. 2005. Mapping behaviorally relevant neural circuits with immediate-early gene expression. *Curr Opin Neurobiol*. 15:599–606.

Guzowski JF, Worley PF. 2001. Cellular compartment analysis of temporal activity by fluorescence in situ hybridization (catFISH). *Curr Protoc Neurosci*. Chapter 1:Unit. 1:8.

Haberly LB. 1985. Neuronal circuitry in olfactory cortex—anatomy and functional implications. *Chemical Senses*. 10:219–238.

Haberly LB, Price JL. 1978. Association and commissural fiber systems of the olfactory cortex of the rat. *J Comp Neurol*. 178:711–740.

Hansen N, Manahan-Vaughan D. 2015. Locus coeruleus stimulation facilitates long-term depression in the dentate gyrus that requires activation of beta-adrenergic receptors. *Cereb Cortex*. 25:1889–1896.

Hargreaves EL, Rao G, Lee I, Knierim JJ. 2005. Major dissociation between medial and lateral entorhinal input to dorsal hippocampus. *Science*. 308:1792–1794.

Heale VR, Vanderwolf CH. 1995. Scopolamine blocks olfaction-induced fast waves but not olfactory evoked potentials in the dentate gyrus. *Behav Brain Res*. 68:57–64.

Heale VR, Vanderwolf CH, Kavaliers M. 1994. Components of weasel and fox odors elicit fast wave bursts in the dentate gyrus of rats. *Behav Brain Res*. 63:159–165.

Heimer L. 1968. *Synaptic distribution of centripetal and centrifugal nerve fibres in olfactory system of rat. An experimental anatomical study*, J Anat. 103:413–432.

Henriksen EJ, Colgin LL, Barnes CA, Witter MP, Moser MB, Moser EI. 2010. Spatial representation along the proximodistal axis of CA1. *Neuron*. 68:127–137.

Hoang TH, Aliane V, Manahan-Vaughan D. 2018. Novel encoding and updating of positional, or directional, spatial cues are processed by distinct hippocampal subfields: evidence for parallel information processing and the "what" stream. *Hippocampus*. 28:315–326.

Howard JD, Plailly J, Grueschow M, Haynes JD, Gottfried JA. 2009. Odor quality coding and categorization in human posterior piriform cortex. *Nat Neurosci*. 12:932–938.

Jacobs LF. 2012. From chemotaxis to the cognitive map: the function of olfaction. *Proc Natl Acad Sci U S A*. 109 Suppl 1:10693–10700.

Jacobs LF, Arter J, Cook A, Sulloway FJ. 2015. Olfactory orientation and navigation in humans. *PLoS One*. 10: e0129387.

Jacobs LF, Menzel R. 2014. Navigation outside of the box: what the lab can learn from the field and what the field can learn from the lab. *Mov Ecol*. 2:3.

Kadohisa M, Wilson DA. 2006. Separate encoding of identity and similarity of complex familiar odors in piriform cortex. *Proc Natl Acad Sci U S A*. 103:15206–15211.

Kay LM, Beshel J. 2010. A beta oscillation network in the rat olfactory system during a 2-alternative choice odor discrimination task. *J Neurophysiol*. 104:829–839.

Kay LM, Beshel J, Brea J, Martin C, Rojas-Libano D, Kopell N. 2009. Olfactory oscillations: the what, how and what for. *Trends Neurosci*. 32:207–214.

Kemp A, Manahan-Vaughan D. 2004. Hippocampal long-term depression and long-term potentiation encode different aspects of novelty acquisition. *Proc Natl Acad Sci U S A*. 101:8192–8197.

Kemp A, Manahan-Vaughan D. 2005. The 5-hydroxytryptamine4 receptor exhibits frequency-dependent properties in synaptic plasticity and behavioural metaplasticity in the hippocampal CA1 region in vivo. *Cereb Cortex*. 15:1037–1043.

Kenney J, Manahan-Vaughan D. 2013. NMDA receptor-dependent synaptic plasticity in dorsal and intermediate hippocampus exhibits distinct frequency-dependent profiles. *Neuropharmacology*. 74:108–118.

Kerr KM, Agster KL, Furtak SC, Burwell RD. 2007. Functional neuroanatomy of the parahippocampal region: the lateral and medial entorhinal areas. *Hippocampus*. 17:697–708.

Klausnitzer J, Kulla A, Manahan-Vaughan D. 2004. Role of the group III metabotropic glutamate receptor in LTP, depotentiation and LTD in dentate gyrus of freely moving rats *Neuropharmacology*. 46:160–170.

Knierim JJ, Neunuebel JP, Deshmukh SS. 2014. Functional correlates of the lateral and medial entorhinal cortex: objects, path integration and local-global reference frames. *Philos Trans R Soc Lond B Biol Sci*. 369: 20130369.

Leitner FC, Melzer S, Lutcke H, Pinna R, Seeburg PH, Helmchen F, Monyer H. 2016. Spatially segregated feedforward and feedback neurons support differential odor processing in the lateral entorhinal cortex. *Nat Neurosci*. 19: 935–944.

Li Y, Xu J, Liu Y, Zhu J, Liu N, Zeng W, Huang N, Rasch MJ, Jiang H, Gu X *et al*. 2017. A distinct entorhinal cortex to hippocampal CA1 direct circuit for olfactory associative learning. *Nat Neurosci*. 20:559–570.

Lyford GL, Yamagata K, Kaufmann WE, Barnes CA, Sanders LK, Copeland NG, Gilbert DJ, Jenkins NA, Lanahan AA, Worley PF. 1995. Arc, a growth factor and activity-regulated gene, encodes a novel cytoskeleton-associated protein that is enriched in neuronal dendrites. *Neuron*. 14:433–445.

Manahan-Vaughan D. 1997. Group 1 and 2 metabotropic glutamate receptors play differential roles in hippocampal long-term depression and long-term potentiation in freely moving rats. *J Neurosci.* 17:3303–3311.

Manahan-Vaughan D. 2000. Long-term depression in freely moving rats is dependent upon strain variation, induction protocol and behavioral state. *Cerebral Cortex.* 10:482–487.

Manahan-Vaughan D. 2018. Recording field potentials and synaptic plasticity from freely behaving rodents. In: Manahan-Vaughan D, editor. *Handbook of in vivo neural plasticity techniques.* Academic Press, London, pp. 1–42

Manahan-Vaughan D, Braunewell KH. 1999. Novelty acquisition is associated with induction of hippocampal long-term depression. *Proc Natl Acad Sci U S A.* 96:8739–8744.

Manahan-Vaughan D, Reymann KG. 1995. Regional and developmental profile of modulation of hippocampal synaptic transmission and LTP by AP4-sensitive mGluRs in vivo. *Neuropharmacology.* 34:991–1001.

Manahan-Vaughan D, Schwegler H. 2011. Strain-dependent variations in spatial learning and in hippocampal synaptic plasticity in the dentate gyrus of freely behaving rats. *Front Behav Neurosci.* 5:7.

Manns JR, Howard MW, Eichenbaum H. 2007. Gradual changes in hippocampal activity support remembering the order of events. *Neuron.* 56:530–540.

Martin C, Beshel J, Kay LM. 2007. An olfacto-hippocampal network is dynamically involved in odor-discrimination learning. *J Neurophysiol.* 98:2196–2205.

Martin C, Gervais R, Chabaud P, Messaoudi B, Ravel N. 2004. Learning-induced modulation of oscillatory activities in the mammalian olfactory system: the role of the centrifugal fibres. *J Physiol Paris.* 98:467–478.

Mouly AM, Fort A, Ben-Boutayab N, Gervais R. 2001. Olfactory learning induces differential long-lasting changes in rat central olfactory pathways. *Neuroscience.* 102:11–21.

Mulisch M, Welsch U. 2010. *Romeis—Mikroskopische Technik.* Spektrum Akademischer Verlag, Heidelberg.

Neves G, Cooke SF, Bliss TV. 2008. Synaptic plasticity, memory and the hippocampus: a neural network approach to causality. *Nat Rev Neurosci.* 9:65–75.

Ohara S, Sato S, Tsutsui K, Witter MP, Iijima T. 2013. Organization of multisynaptic inputs to the dorsal and ventral dentate gyrus: retrograde trans-synaptic tracing with rabies virus vector in the rat. *PLoS One.* 8: e78928.

Paxinos G, Watson C. 1998. *The rat brain in stereotaxic coordinates.* San Diego: Academic Press

Paxinos G, Watson C. 2005. *The rat brain in stereotaxic coordinates.* Amsterdam; Boston: Elsevier Academic Press

Petrulis A, Alvarez P, Eichenbaum H. 2005. Neural correlates of social odor recognition and the representation of individual distinctive social odors within entorhinal cortex and ventral subiculum. *Neuroscience.* 130:259–274.

Price JL. 1973. An autoradiographic study of complementary laminar patterns of termination of afferent fibers to the olfactory cortex. *J Comp Neurol.* 150:87–108.

Racine RJ, Milgram NW, Hafner S. 1983. Long-term potentiation phenomena in the rat limbic forebrain. *Brain Res.* 260:217–231.

Rangel LM, Rueckemann JW, Riviere PD, Keefe KR, Porter BS, Heimbuch IS, Budlong CH, Eichenbaum H. 2016. Rhythmic coordination of hippocampal neurons during associative memory processing. *Elife.* 5: e09849.

Ravel N, Chabaud P, Martin C, Gaveau V, Hugues E, Tallon-Baudry C, Bertrand O, Gervais R. 2003. Olfactory learning modifies the expression of odour-induced oscillatory responses in the gamma (60–90 Hz) and beta (15–40 Hz) bands in the rat olfactory bulb. *Eur J Neurosci.* 17:350–358.

Sauvage MM, Nakamura NH, Beer Z. 2013. Mapping memory function in the medial temporal lobe with the immediate-early gene arc. *Behav Brain Res.* 254:22–33.

Schaefer LH, Schuster D, Schaffer J. 2004. Structured illumination microscopy: artefact analysis and reduction utilizing a parameter optimization approach. *J Microsc.* 216:165–174.

Sosulski DL, Bloom ML, Cutforth T, Axel R, Datta SR. 2011. Distinct representations of olfactory information in different cortical centres. *Nature.* 472:213–216.

Squire LR. 1992. Memory and the hippocampus: a synthesis from findings with rats, monkeys, and humans. *Psychol Rev.* 99:195–231.

Squire LR, Stark CE, Clark RE. 2004. The medial temporal lobe. *Annu Rev Neurosci.* 27:279–306.

Strauch C, Manahan-Vaughan D. 2018. In the piriform cortex, the primary impetus for information encoding through synaptic plasticity is provided by descending rather than ascending olfactory inputs. *Cereb Cortex.* 28:764–776.

Tamamaki N. 1997. Organization of the entorhinal projection to the rat dentate gyrus revealed by Dil anterograde labeling. *Exp Brain Res.* 116:250–258.

Thiels E, Barrionuevo G, Berger TW. 1994. Excitatory stimulation during postsynaptic inhibition induces long-term depression in hippocampus in vivo. *J Neurophysiol.* 72:3009–3016.

Thiels E, Xie X, Yeckel MF, Barrionuevo G, Berger TW. 1996. NMDA receptor-dependent LTD in different subfields of hippocampus in vivo and in vitro. *Hippocampus.* 6:43–51.

Truchet B, Chaillan FA, Soumireu-Mourat B, Roman FS. 2002. Learning and memory of cue-reward association meaning by modifications of synaptic efficacy in dentate gyrus and piriform cortex. *Hippocampus.* 12:600–608.

Tsanov M, Manahan-Vaughan D. 2009. Visual cortex plasticity evokes excitatory alterations in the hippocampus. *Front Integr Neurosci.* 3:32.

Vanderwolf CH. 1992. Hippocampal activity, olfaction, and sniffing: an olfactory input to the dentate gyrus. *Brain Res.* 593:197–208.

Vazdarjanova A, McNaughton BL, Barnes CA, Worley PF, Guzowski JF. 2002. Experience-dependent coincident expression of the effector immediate-early genes arc and Homer 1a in hippocampal and neocortical neuronal networks. *J Neurosci.* 22:10067–10071.

Wiescholleck V, Manahan-Vaughan D. 2014. Antagonism of D1/D5 receptors prevents long-term depression (LTD) and learning-facilitated LTD at the perforant path-dentate gyrus synapse in freely behaving rats. *Hippocampus.* 24:1615–1622.

Witter MP, Doan TP, Jacobsen B, Nilssen ES, Ohara S. 2017. Architecture of the entorhinal cortex a review of entorhinal anatomy in rodents with some comparative notes. *Front Syst Neurosci.* 11:46.

Witter MP, Wouterlood FG, Naber PA, Van Haeften T. 2000. Anatomical organization of the parahippocampal-hippocampal network. *Ann N Y Acad Sci.* 911:1–24.

Wyss JM. 1981. An autoradiographic study of the efferent connections of the entorhinal cortex in the rat. *J Comp Neurol.* 199:495–512.

Zelcer I, Cohen H, Richter-Levin G, Lebiosn T, Grossberger T, Barkai E. 2006. A cellular correlate of learning-induced metaplasticity in the hippocampus. *Cereb Cortex.* 16:460–468.

Zhang S, Manahan-Vaughan D. 2015. Spatial olfactory learning contributes to place field formation in the hippocampus. *Cereb Cortex.* 25:423–432.